

pubs.acs.org/JACS Communication

Chiral Bifunctional Phosphine Ligand-Enabled Cooperative Cu Catalysis: Formation of Chiral α,β -Butenolides via Highly Enantioselective γ -Protonation

Xinpeng Cheng, Tianyou Li, Kaylaa Gutman, and Liming Zhang*



Cite This: J. Am. Chem. Soc. 2021, 143, 10876-10881



ACCESS I

III Metrics & More

Article Recommendations

Supporting Information

ABSTRACT: α,β -Butenolides with \geq 96% enantiomeric excess are synthesized from β,γ -butenolides via a novel Cu(I)-ligand cooperative catalysis. The reaction is enabled by a chiral biphenyl-2-ylphosphine ligand featuring a remote tertiary amino group. Density functional theory studies support the cooperation between the metal center and the ligand basic amino group during the initial soft deprotonation and the key asymmetric γ -protonation. Remarkably, other coinage metals, that is, Ag and Au, can readily assume the same role as Cu in this asymmetric isomerization chemistry.

Scheme 1. Butenolide Natural Product and Reaction Design

A. Natural products containing the α,β-butenolide core structure

Me

Me

AcO

H

Me

Me

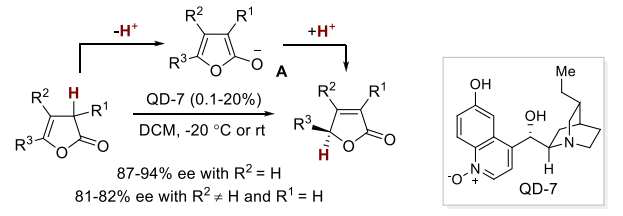
Avenolide

Avenolide

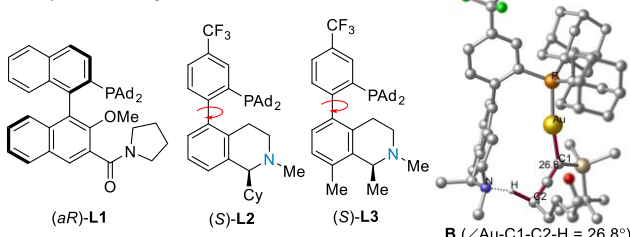
Thorectandrols B

Kallolide A

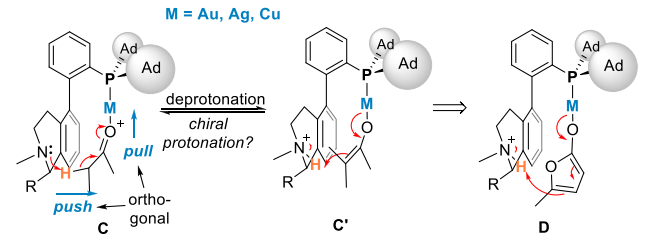
B. Prior work by Deng on asymmmetric isomerzation of β , γ -butenolides



C. Chiral bifunctional ligands developed for asymmetric gold-ligand cooperative catalysis



D. Ligand-enabled soft enolization



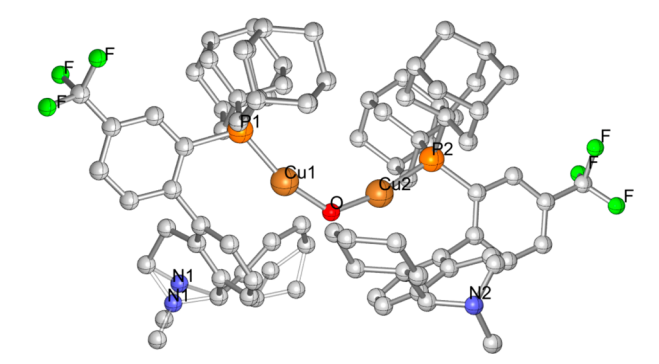


Figure 1. CYL drawing of the dimeric Cu(I) complex. The crystal solvent molecules, that is, one MeCN and three Et_2O , are omitted for clarity. $\angle P1-Cu1-O=163.2^{\circ}$ and $\angle P2-Cu2-O=167.8^{\circ}$.

any natural products featuring chiral α,β -butenolide motifs possess various biological activities (Scheme 1A). For example, avenolide can control the production of antibiotics in *Streptomyces avermitilis*, ¹ thorectandrols B inhibits the growth of MALME-3 M (melanoma) and MCF-7 (breast) cancer cell lines, ² and kallolide A exhibits anti-inflammatory activity. ³ Various synthetic approaches have been developed to access chiral α,β -butenolide. ⁴ The direct catalytic olefin isomerization of racemic/achiral β,γ -butenolide into chiral α,β -butenolide via the achiral 2-furanoxyl anion A is an atom-economic and arguably the simplest approach (Scheme 1B), yet it has been only sparsely explored. A notable advance in this strategy was achieved by Deng ⁵ in 2011 by employing a cinchona-derived

Received: June 4, 2021 Published: July 15, 2021





Table 1. Reaction Condition Optimization

entry ^a	catalyst	time (h)	conv.	yield (%) ^b	ee (%) ^c
1	[Cu(MeCN) ₄] ⁺ PF ₆ ⁻	3	2	NA	NA
2	$[Cu(MeCN)_4]^+ PF_6^- /Et_3N$	3	3	NA	NA
3	[JohnPhosCu(MeCN)] ⁺ PF ₆ ⁻ /Et ₃ N	16	35	6	NA
4	[Cu(MeCN) ₄] ⁺ PF ₆ ⁻ /L4	3	100	99	NA
5	$[Cu(MeCN)_4]^+ PF_6^- / (S)-L2$	3	100	99	98
6	$[Cu(MeCN)_4]^+ PF_6^- / (S)-L3$	3	100	99	94
7	$[(S)-L2Cu(MeCN)]^+ PF_6^-$	1	100	99	97
8^d	$[(S)-L2Cu(MeCN)]^+PF_6^-$	0.5	100	99 ^e	98
$9^{d,f}$	$\{[(S)-L2Cu]_2(H_2O)\}^{2+}(PF_6^-)_2$	0.5	100	99	98
10	(S)-L2	3	NA	NA	NA
11	$Cu(OTf)_2$ or $Cu(hfac)_2/(S)$ -L2	24	<5	<5	NA
12	(S)-L2AuCl/NaBAr ^F ₄ (10 mol %)	0.5	100	99	99
13	$[Ag(MeCN)_{2}]^{+}BAr_{4}^{F_{-}}/(S)-L2$	0.5	100	99	98
14 ^g	$[(S)-L2Cu(MeCN)]^+ PF_6^-$	1	100	92 ^h	99

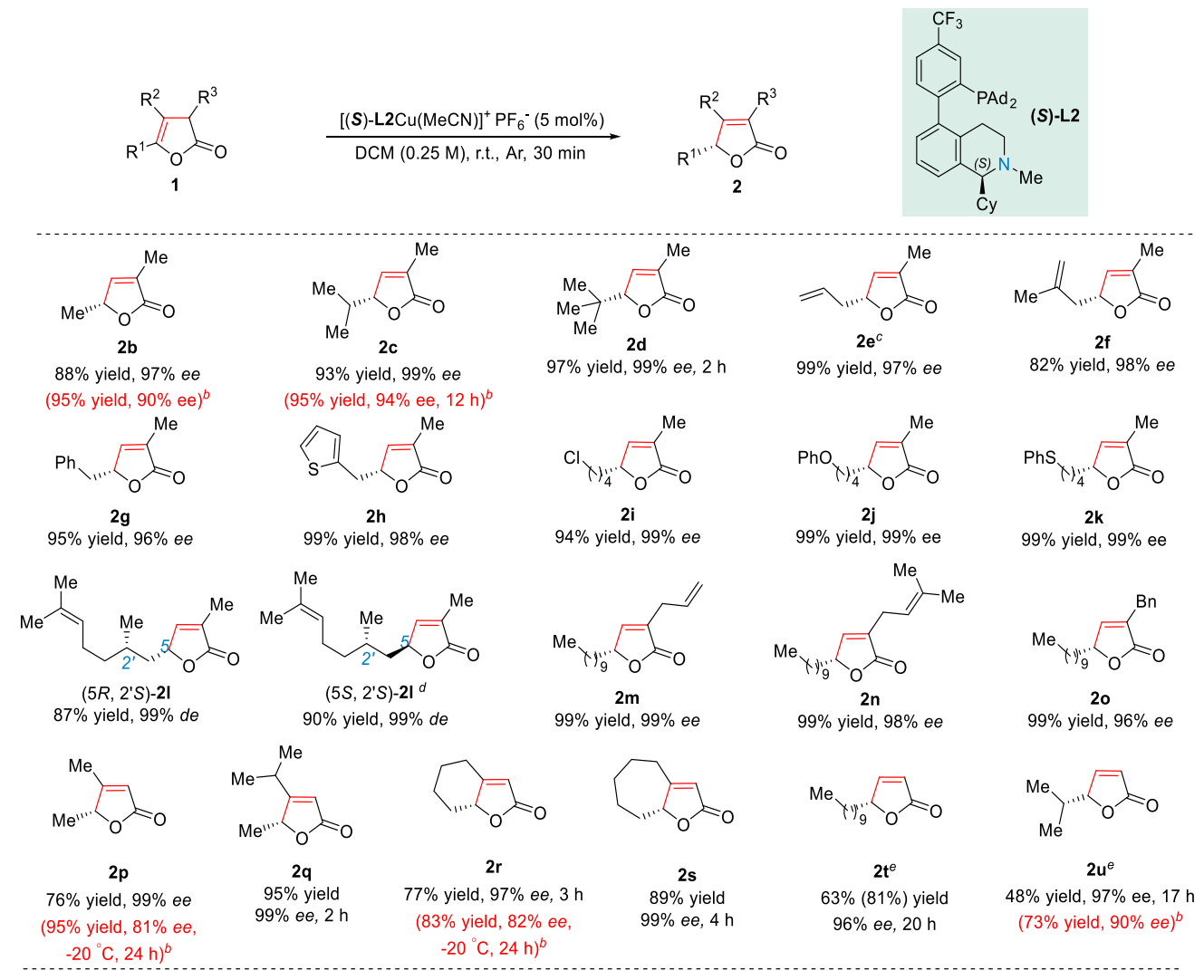
 a Reaction was performed at 0.05 mmol scale in 1-dram vials. b NMR yield is calculated by assuming that the triplet at around 0.87 ppm corresponds to the terminal methyl groups of all compounds. c Detected using chiral HPLC. d Under Ar atmosphere. e Isolated yield. f Reaction was performed with 2.5 mol % catalyst. g Reaction was performed with 1 mol %. h 0.99 g product isolated.

organocatalyst. In this chemistry, good levels of enantioselectivities (87–94% ee) are achieved for γ -monosubstituted and α , γ -disubstituted α , β -butenolide products, but only moderate ee values (81–82%) are reported for the β , γ -disubstituted α , β -butenolides. This chemistry was applied in the total synthesis of Leucosceptroid family of natural products, where a moderate diastereomeric ratio of 7:1 was reported with the latter butenolide type. Herein, we report a Cu(I)-bifunctional phosphine cooperative catalysis that achieves the asymmetric butenolide isomerization, which exhibits enantiomeric excess ranging from 96–99%. Moreover, this chemistry is applicable to all of the three aforementioned substitution patterns and proceeds at ambient temperature and reaches completion mostly in 0.5 h.

For the past several years, we⁷ have developed various bifunctional biphenyl-2-ylphosphine ligands⁸ featuring a remote basic group for gold-ligand cooperative catalysis.^{8,9} Scheme 1C shows the chiral ligands that have enabled asymmetric cooperative gold catalysis. 8a,c,e Among them, L2 and L3 feature a fluxional biphenyl axis and a remote tertiary amino group possessing an α -chiral center and engaging in critical propargylic deprotonation during catalysis, as revealed by the density functional theory (DFT)-optimized TS B using (S)-L3 as the ligand. 8e Despite the syn-periplanar nature of the concerted Auactivation and amino-deprotonation, we envisioned that an orthogonal organization of a "pulling" cationic metal and a "pushing" basic amino group can be readily achieved by these chiral ligands, as outlined in the structures C and C' in Scheme 1D, which should be suited for soft enolization and the reverse protonation. This protonation of the metal enolate could be extended to the γ -protonation of the metal 2-furanolate in **D**. As such, we envision that chiral ligands such as L2 or L3 might enable highly enantioselective isomerization of $\beta_1 \gamma$ -butenolides via sequential soft enolization and asymmetric γ -protonation.¹⁰ Since Cu(I) and Ag(I) can adopt the same linear biscoordinated structures with bulky phosphine as $\operatorname{Au}(I)$, ¹¹ we anticipate that the corresponding $\operatorname{Cu}(I)$ or $\operatorname{Ag}(I)$ complexes featuring these bifunctional ligands could also be effective in this cooperative catalysis manifold. ¹² Moreover, these harder and cheaper coinage metals may be advantageous in enolate chemistry over softer Au since the coordination/activation of hard carbonyl oxygen instead of soft $\operatorname{C-C}$ triple bond is desired. It is noteworthy that metal—ligand cooperative catalysis involving $\operatorname{Cu}(I)^{13}$ or $\operatorname{Ag}(I)$ is scarce, and this design, if implemented, would constitute the first application of this class of bifunctional ligands in Cu or Ag catalysis.

Guided by these considerations, we initiated our investigation by employing Cu as the metal and the β , γ -butenolide 1a, prepared from an allenic ester in two steps,⁵ as the model substrate. As expected, the Cu^{I} salt, $[Cu(MeCN)_{4}]^{+} PF_{6}^{-}$, alone could not promote the isomerization of 1a into the α,β butenolide product 2a to a noticeable extent (entry 1) nor was its combination with Et₃N (entry 2). [JohnPhosCu(MeCN)]⁺ PF₆^{-11b} and Et₃N (5 mol % each) did lead to substantial conversion in 16 h at ambient temperature, albeit in 6% yield (entry 3). The reaction was, however, drastically improved when JohnPhos was replaced by the achiral tertiary amine-functionalized ligand L4.8b With the in situ generated L4Cu+, the reaction reached completion in 3 h and afforded 2a in nearly quantitative yield (entry 4). This large enhancement of reactivity is consistent with the intended Cu-ligand cooperation. When the chiral ligand (S)-L2 along with [Cu(MeCN)₄]⁺ PF₆⁻ was employed, the reaction again proceeded with excellent efficiency, and moreover, the ee of 2a was 98% (entry 5). The (R)-configuration of 2a is inferred by comparing the specific optical rotations of its homologues 2b and 2c (see Table 2) with the literature data. The replacement of (S)-L2 with (S)-L3^{8e} led to 94% ee (entry 6). To establish the structure of the Cu(I) catalyst, we prepared $[(S)-L2Cu(MeCN)]^+ PF_6^-$ by following the related protocol for ['BuXPhosCu(MeCN)]+BF₄-. 11b With

Table 2. Reaction Scope^a



^aReaction was performed in 2-dram sealed vials under argon at room temperature. Yield calculated based on the conversation was included in parentheses. Reaction scale is 0.3 mmol and reaction time is 0.5 h if not specified. ^bResult reported in ref 5. ^cReaction was performed at 0.15 mmol scale. ^d5 mol % (R)-L2Cu(MeCN)PF₆ was used. ^cReaction was performed at 40 °C.

this preformed chiral cationic Cu(I) complex as the catalyst, the reaction time was shortened to 1 h, while the yield and ee remained excellent (entry 7). Performing the reaction under argon atmosphere further shortened the reaction time to 30 min (entry 8). This observation is consistent with Cu(I) catalysis as atmospheric oxygen might oxidize Cu(I) to likely nonreactive Cu(II). To further characterize the Cu(I) catalyst, we obtained its single crystals for X-ray diffraction studies. However, the solved structure, as shown in Figure 1, is a dimeric (S)-L2Cu(I) complex with the two-metal center bridged by a molecule of water. Nevertheless, it confirms that the Cu(I) center is biscoordinated, with the angles of P-Cu-O being 167.8° and 163.2°, respectively. This structural feature supports our reaction design. Moreover, this dimeric complex is equally effective as the catalyst (entry 9). In the control experiments, the ligand itself was not competent (entry 10), and Cu(II) salts such as Cu(OTf)₂ and Cu(hfac)₂ could not serve as the copper source (entry 11). Interestingly, this catalytic system worked equally well with the other coinage metals. Hence, with Ag(I) or Au(I) at the metal center, nearly identical results were obtained

(entries 12 and 13). This interchangeability among the coinage metals is remarkable and rare. The scalability of this Cu(I) catalysis was demonstrated on a gram-scale reaction in entry 14. With 1 mol % of the catalyst, the reaction reached completion in 1 h and delivered 0.99 g of 2a in 92% yield and with 99% ee.

With the optimized reaction conditions (i.e., Table 1, entry 8) in hand, we set out to explore the reaction scope. As shown in Table 2, a series of α, γ -disubstituted α, β -butenolides ($2\mathbf{b}-2\mathbf{o}$) were synthesized in yields ranging from 88-99% and with $\geq 96\%$ ee. The \mathbb{R}^1 group in this series can accommodate methyl ($2\mathbf{b}$), isopropyl ($2\mathbf{c}$), bulky t-butyl group ($2\mathbf{d}$), and various functional groups including $\mathbb{C}-\mathbb{C}$ double bonds ($2\mathbf{e}$ and $2\mathbf{f}$), phenyl ($2\mathbf{g}$), thiophen-2-yl ($2\mathbf{h}$), chloro ($2\mathbf{i}$), phenyloxy ($2\mathbf{j}$), and phenylthio ($2\mathbf{k}$). From the substrate prepared from (S)- β -citronellol, (SS, 2'S)- $2\mathbf{l}$ was formed with 99% diastereomeric excess when (S)- $\mathbf{L}2$ was employed. By switching the chiral ligand to its enantiomer, the diastereomer (SS, SS)-SS1 was formed with the same level of excellent diastereoselectivity. This ligand-enabled diastereomeric divergence permits flexible and selective access to stereochemical arrays. Little impact on the reactivities

Scheme 2. DFT Calculated Energetics of the Reaction Forming 2b at the PBE1PBE/6-31(d,p)/6-311g(d,p)(P)/SDD(Cu) Level of Theory with SMD (DCM)

was noticed when the R^3 group was switched from methyl (2a) to allyl (2m), prenyl (2n), or benzyl (2o).

Next, we turned our attention to the synthesis of $\beta_1 \gamma$ -disubstituted $\alpha_1 \beta$ -butenolides (2p-2s). Much to our delight, they were also formed with \geq 97% ee. The β -substituent, R^2 , can be sterically demanding isopropyl (2q) or part of 6-/7-membered ring connected to the γ substituent (2r and 2s).

Finally, the preparation of chiral monosubstituted α,β -butenolides (2t and 2u) was examined. As expected, in the absence of α - or β -substituents to stabilize the product double bond, the energy differences between the substrates and the products appear to be small. As such, this asymmetric isomerization was sluggish and could not reach full conversion due to reaction equilibrium. The slightly forcing conditions, i.e., 40 °C and 17 h, were employed to improve the reaction yields without compromising the exceptional enantioselectivity. Because of volatility, the isolated yield of 2u was moderate.

In comparison to literature results, 5 which are shown in red in Table 2, this asymmetric Cu(I) catalysis displays marked improvement in asymmetric induction. The difference is particularly significant in the cases of the β , γ -disubstituted α , β -butenolides **2p** and **2r**, where the *ee* values were improved from 81% to 99% and from 82% to 97%, respectively. Moreover, the reaction conditions were substantially improved, that is, rt and 0.5–3 h over –20 °C and 24 h.

The NMR spectra of $[(S)\text{-L2Cu}(\text{MeCN})]^+$ PF₆⁻ in CD₂Cl₂ under ambient conditions revealed a ~1:1 mixture of atropisomers, which was caused by the retarded rotation of its biphenyl axis. In the atropisomer with the axis configuration identical to those in the X-ray structure in Figure 1, the ligand nitrogen lone pair electrons point away from the metal center or are shielded by the α -cyclohexyl group. As such, it is not catalytically active. We determined by NMR that the coalescence of the atropisomeric chemical shifts of this Cu(I) complex occurred between 60 and 65 °C and the rotational barrier was calculated to be 17.8–18.1 kcal/mol. At ambient temperature, the biphenyl axis is sufficiently fluxional and most of the catalyst should participate in the catalysis by adopting the

desired axis configuration. We also examined the correlation between the ee of 2a and the ee of $[L2Cu(MeCN)]^+$ PF_6^- . A moderate negative nonlinear effect was revealed (see Supporting Information). This phenomenon can be interpreted as the monomeric Cu(I) complex being the active catalyst and equilibrating homochiral dimeric/polymeric Cu(I) species such as $\{[(S)-L2Cu]_2\cdot H_2O\}^{2+}$ $(PF_6^-)_2$ being catalytically incompetent. The support of $[(S)-L2Cu]_2\cdot H_2O\}^{2+}$ $(PF_6^-)_2$ being catalytically incompetent.

To offer insight into the reaction mechanism and understand the extraordinary asymmetric induction, we conducted DFT studies of the reaction forming 2b at the PBE1PBE level using the effective core potential SDD for Cu and the basis set 6-311g(d,p) for P and 6-31g(d,p) for the other atoms. The SMD model is employed for solvent DCM. As shown in Scheme 2, the deprotonation step eliminates the α -chiral center of the $\beta_i \gamma$ butenolide 1b and exhibits only a minor difference in reaction barriers. The dihedral angles of Cu–O1–C α -H in the transition states for the (S)- and (R)-1b substrates, a measure of the relative orientation of the "push" and "pull" in this soft enolization, are 46.9° and 72.5°, respectively, revealing deviation from orthogonality but supporting the cooperative nature of the metal and the ligand amino group in the deprotonation process. The formed (furan-2-yloxy)copper(I) intermediates 3-L2Cu and 3-L2Cu' are conformers and differ little in free energy. The subsequent γ -protonation generates the butenolide γ -chiral center and the two TS differ in free energy by 7.7 kcal/mol, which is consistent with the observed excellent ee (i.e., 97%). In the favored TS structure TS-(R)-2b-L2Cu leading to the observed (R)-2b, the dihedral angle of Cu-O1-C γ -H is 67.6°, while that for the disfavored TS is 1.1°. This stark difference in the relative orientation of Cu–O1 and Cγ-H reveals the former achieving substantially better metal-ligand cooperation and is attributed to the difference in reaction energy barriers. Additionally, the energy barrier of the preferred protonation is lower than that of deprotonating either of the 1b enantiomers by \geq 2.3 kcal/mol, suggesting that the stereoeliminating deprotonation is the rate-limiting step, which is opposite to that revealed by DFT studies of the Deng's chemistry.

In summary, we have developed a rare Cu(I)-ligand cooperative catalysis that is enabled by a chiral bifunctional biphenyl-2-ylphosphine ligand. The reaction converts three types of β , γ -butenolides into chiral α , β -butenolides with \geq 96% ee. DFT calculations support the cooperative nature between the Cu(I) center and the ligand remote amino group in both the soft deprotonation and the asymmetric γ -protonation steps. Remarkably, other coinage metals, that is, Ag and Au, can be equally effective in this catalysis. We anticipate that this coinage metal—ligand cooperation approach would find broader applications in asymmetric protonation and enolate chemistry.

ASSOCIATED CONTENT

Supporting Information

The Supporting Information is available free of charge at https://pubs.acs.org/doi/10.1021/jacs.1c05781.

Experimental procedures and characterization data, computational study results, Cartesian coordinates, spectral data (PDF)

Accession Codes

CCDC 2052076 contains the supplementary crystallographic data for this paper. These data can be obtained free of charge via www.ccdc.cam.ac.uk/data_request/cif, or by emailing data_request@ccdc.cam.ac.uk, or by contacting The Cambridge Crystallographic Data Centre, 12 Union Road, Cambridge CB2 1EZ, UK; fax: +44 1223 336033.

AUTHOR INFORMATION

Corresponding Author

Liming Zhang — Department of Chemistry and Biochemistry, University of California, Santa Barbara, Santa Barbara, California 93106, United States; orcid.org/0000-0002-5306-1515; Email: zhang@chem.ucsb.edu

Authors

Xinpeng Cheng – Department of Chemistry and Biochemistry, University of California, Santa Barbara, Santa Barbara, California 93106, United States

Tianyou Li – Department of Chemistry and Biochemistry, University of California, Santa Barbara, Santa Barbara, California 93106, United States

Kaylaa Gutman — Department of Chemistry and Biochemistry, University of California, Santa Barbara, Santa Barbara, California 93106, United States

Complete contact information is available at: https://pubs.acs.org/10.1021/jacs.1c05781

Notes

The authors declare no competing financial interest.

ACKNOWLEDGMENTS

The authors thank NIH R01GM123342 and 1R35GM139640 and NSF CHE 1800525 for financial support, NSF MRI-1920299 for the acquisition of Bruker 500 and 400 MHz NMR instruments, and Drs. Ting Li and Conghui Tang for conducting some initial studies on the related gold catalysis. CNS-1725797 and DMR 1720256 are also acknowledged.

■ REFERENCES

(1) (a) Kitani, S.; Miyamoto, K. T.; Takamatsu, S.; Herawati, E.; Iguchi, H.; Nishitomi, K.; Uchida, M.; Nagamitsu, T.; Omura, S.; Ikeda, H.; Nihira, T. Avenolide, a *Streptomyces* Hormone Controlling

Antibiotic Production in *Streptomyces Avermitilis*. *Proc. Natl. Acad. Sci. U. S. A.* **2011**, *108*, 16410–16415. (b) Uchida, M.; Takamatsu, S.; Arima, S.; Miyamoto, K. T.; Kitani, S.; Nihira, T.; Ikeda, H.; Nagamitsu, T. Total Synthesis and Absolute Configuration of Avenolide, Extracellular Factor in Streptomyces Avermitilis. *J. Antibiot.* **2011**, *64*, 781–787

- (2) Charan, R. D.; McKee, T. C.; Boyd, M. R. Thorectandrols a and B, New Cytotoxic Sesterterpenes from the Marine Sponge Thorectandra Species. *J. Nat. Prod.* **2001**, *64*, 661–663.
- (3) (a) Look, S. A.; Burch, M. T.; Fenical, W.; Zheng, Q.; Clardy, J. Kallolide a, a New Antiinflammatory Diterpenoid, and Related Lactones from the Caribbean Octocoral Pseudopterogorgia Kallos (Bielschowsky). *J. Org. Chem.* 1985, 50, 5741–5746. (b) Marshall, J. A.; Liao, J. Stereoselective Total Synthesis of the Pseudopterolide Kallolide A. *J. Org. Chem.* 1998, 63, 5962–5970.
- (4) (a) Carter, N. B.; Nadany, A. E.; Sweeney, J. B. Recent Developments in the Synthesis of Furan-2(5h)-Ones. *J. Chem. Soc, Perkin Trans.* 1 2002, 2324–2342. (b) Mao, B.; Fañanás-Mastral, M.; Feringa, B. L. Catalytic Asymmetric Synthesis of Butenolides and Butyrolactones. *Chem. Rev.* 2017, 117, 10502–10566.
- (5) Wu, Y.; Singh, R. P.; Deng, L. Asymmetric Olefin Isomerization of Butenolides Via Proton Transfer Catalysis by an Organic Molecule. *J. Am. Chem. Soc.* **2011**, 133, 12458–12461.
- (6) Hugelshofer, C. L.; Magauer, T. Total Synthesis of the Leucosceptroid Family of Natural Products. *J. Am. Chem. Soc.* **2015**, 137, 3807–3810.
- (7) Cheng, X.; Zhang, L. Designed Bifunctional Ligands in Cooperative Homogeneous Gold Catalysis. *CCS Chem.* **2021**, 2, 1989–2002.
- (8) (a) Cheng, X.; Wang, Z.; Quintanilla, C. D.; Zhang, L. Chiral Bifunctional Phosphine Ligand Enabling Gold-Catalyzed Asymmetric Isomerization of Alkyne to Allene and Asymmetric Synthesis of 2,5-Dihydrofuran. J. Am. Chem. Soc. 2019, 141, 3787-3791. (b) Wang, Z.; Ying, A.; Fan, Z.; Hervieu, C.; Zhang, L. Tertiary Amino Group in Cationic Gold Catalyst: Tethered Frustrated Lewis Pairs That Enable Ligand-Controlled Regiodivergent and Stereoselective Isomerizations of Propargylic Esters. ACS Catal. 2017, 7, 3676-3680. (c) Wang, Z.; Nicolini, C.; Hervieu, C.; Wong, Y.-F.; Zanoni, G.; Zhang, L. Remote Cooperative Group Strategy Enables Ligands for Accelerative Asymmetric Gold Catalysis. J. Am. Chem. Soc. 2017, 139, 16064-16067. (d) Wang, Y.; Wang, Z.; Li, Y.; Wu, G.; Cao, Z.; Zhang, L. A General Ligand Design for Gold Catalysis Allowing Ligand-Directed Anti-Nucleophilic Attack of Alkynes. Nat. Commun. 2014, 3470. (e) Li, T.; Cheng, X.; Qian, P.; Zhang, L. Gold-Catalysed Asymmetric Net Addition of Unactivated Propargylic C-H Bonds to Tethered Aldehydes. Nat. Catal. 2021, 4, 164-171. (f) Wang, Z.; Wang, Y.; Zhang, L. Soft Propargylic Deprotonation: Designed Ligand Enables Au-Catalyzed Isomerization of Alkynes to 1,3-Dienes. J. Am. Chem. Soc. 2014, 136, 8887-8890.
- (9) (a) Li, T.; Zhang, L. Bifunctional Biphenyl-2-Ylphosphine Ligand Enables Tandem Gold-Catalyzed Propargylation of Aldehyde and Unexpected Cycloisomerization. J. Am. Chem. Soc. 2018, 140, 17439-17443. (b) Zhang, J.-Q.; Liu, Y.; Wang, X.-W.; Zhang, L. Synthesis of Chiral Bifunctional Nhc Ligands and Survey of Their Utilities in Asymmetric Gold Catalysis. Organometallics 2019, 38, 3931-3938. (c) Wang, H.; Li, T.; Zheng, Z.; Zhang, L. Efficient Synthesis of A-Allylbutenolides from Allyl Ynoates Via Tandem Ligand-Enabled Au(I) Catalysis and the Claisen Rearrangement. ACS Catal. 2019, 9, 10339-10342. (d) Cheng, X.; Quintanilla, C. D.; Zhang, L. Total Synthesis and Structure Revision of Diplobifuranylone B. J. Org. Chem. 2019, 84, 11054-11060. (e) Liao, S.; Porta, A.; Cheng, X.; Ma, X.; Zanoni, G.; Zhang, L. Bifunctional Ligand Enables Efficient Gold-Catalyzed Hydroalkenylation of Propargylic Alcohol. Angew. Chem., Int. Ed. 2018, 57, 8250-8254. (f) Li, X.; Wang, Z.; Ma, X.; Liu, P.-n.; Zhang, L. Designed Bifunctional Phosphine Ligand-Enabled Gold-Catalyzed Isomerizations of Ynamides and Allenamides: Stereoselective and Regioselective Formation of 1-Amido-1,3-Dienes. Org. Lett. 2017, 19, 5744-5747. (g) Li, X.; Liao, S.; Wang, Z.; Zhang, L. Ligand-Accelerated Gold-Catalyzed Addition of in Situ Generated Hydrazoic

Acid to Alkynes under Neat Conditions. Org. Lett. 2017, 19, 3687–3690.

- (10) (a) Oudeyer, S.; Brière, J.-F.; Levacher, V. Progress in Catalytic Asymmetric Protonation. Eur. J. Org. Chem. 2014, 2014, 6103–6119. (b) Fu, N.; Zhang, L.; Luo, S. Catalytic Asymmetric Enamine Protonation Reaction. Org. Biomol. Chem. 2018, 16, 510–520. (c) Kingston, C.; James, J.; Guiry, P. J. Development of and Recent Advances in Pd-Catalyzed Decarboxylative Asymmetric Protonation. J. Org. Chem. 2019, 84, 473–485. (d) Phelan, J. P.; Ellman, J. A. Conjugate Addition—Enantioselective Protonation Reactions. Beilstein J. Org. Chem. 2016, 12, 1203–1228.
- (11) (a) Grirrane, A.; Álvarez, E.; García, H.; Corma, A. Catalytic Activity of Cationic and Neutral Silver(I)—Xphos Complexes with Nitrogen Ligands or Tolylsulfonate for Mannich and Aza-Diels—Alder Coupling Reactions. *Chem. Eur. J.* 2016, 22, 340–354. (b) Pérez-Galán, P.; Delpont, N.; Herrero-Gómez, E.; Maseras, F.; Echavarren, A. M. Metal—Arene Interactions in Dialkylbiarylphosphane Complexes of Copper, Silver, and Gold. *Chem. Eur. J.* 2010, 16, 5324–5332.
- (12) (a) Higashi, T.; Kusumoto, S.; Nozaki, K. Cleavage of Si–H, B–H, and C–H Bonds by Metal–Ligand Cooperation. *Chem. Rev.* **2019**, 119, 10393–10402. (b) Khusnutdinova, J. R.; Milstein, D. Metal–Ligand Cooperation. *Angew. Chem., Int. Ed.* **2015**, 54, 12236–12273. (c) Gunanathan, C.; Milstein, D. Metal–Ligand Cooperation by Aromatization–Dearomatization: A New Paradigm in Bond Activation and "Green" Catalysis. *Acc. Chem. Res.* **2011**, 44, 588–602.
- (13) (a) Guo, J.; Mao, J. Asymmetric Henry Reaction Catalyzed by Bifunctional Copper-Based Catalysts. Chirality 2009, 21, 619-627. (b) Lang, K.; Park, J.; Hong, S. Development of Bifunctional Aza-Bis(Oxazoline) Copper Catalysts for Enantioselective Henry Reaction. J. Org. Chem. 2010, 75, 6424-6435. (c) Boobalan, R.; Lee, G.-H.; Chen, C. Copper Complex of Aminoisoborneol Schiff Base Cu2(Sbaib-D)2: An Efficient Catalyst for Direct Catalytic Asymmetric Nitroaldol (Henry) Reaction. Adv. Synth. Catal. 2012, 354, 2511-2520. (d) Zhao, L.; Ma, Y.; Duan, W.; He, F.; Chen, J.; Song, C. Asymmetric β -Boration of $\alpha_1\beta$ -Unsaturated N-Acyloxazolidinones by [2.2] Paracyclophane-Based Bifunctional Catalyst. Org. Lett. 2012, 14, 5780-5783. (e) Caron, A.; Morin, É.; Collins, S. K. Bifunctional Copper-Based Photocatalyst for Reductive Pinacol-Type Couplings. ACS Catal. 2019, 9, 9458-9464. (f) Das, S.; Sinha, S.; Samanta, D.; Mondal, R.; Chakraborty, G.; Brandao, P.; Paul, N. D. Metal-Ligand Cooperative Approach to Achieve Dehydrogenative Functionalization of Alcohols to Quinolines and Quinazolin-4(3h)-Ones under Mild Aerobic Conditions. J. Org. Chem. 2019, 84, 10160-10171.
- (14) Satyanarayana, T.; Abraham, S.; Kagan, H. B. Nonlinear Effects in Asymmetric Catalysis. *Angew. Chem., Int. Ed.* **2009**, *48*, 456–494.
- (15) Kina, A.; Iwamura, H.; Hayashi, T. A Kinetic Study on Rh/Binap-Catalyzed 1,4-Addition of Phenylboronic Acid to Enones: Negative Nonlinear Effect Caused by Predominant Homochiral Dimer Contribution. J. Am. Chem. Soc. 2006, 128, 3904—3905.
- (16) Xue, X.-S.; Li, X.; Yu, A.; Yang, C.; Song, C.; Cheng, J.-P. Mechanism and Selectivity of Bioinspired Cinchona Alkaloid Derivatives Catalyzed Asymmetric Olefin Isomerization: A Computational Study. J. Am. Chem. Soc. 2013, 135, 7462–7473.